ACS APPLIED MATERIALS & INTERFACES

Research Article

www.acsami.org

Nanocomposite of N-Doped TiO_2 Nanorods and Graphene as an Effective Electrocatalyst for the Oxygen Reduction Reaction

Wenjing Yuan,[†] Juchuan Li,[‡] Likun Wang,[†] Ping Chen,*[,†] Anjian Xie,[†] and Yuhua Shen*[,†]

[†]School of Chemistry and Chemical Engineering, Anhui University, Hefei, Anhui 230601, P. R. China

[‡]Department of Chemical and Materials Engineering, University of Kentucky, Lexington, Kentucky 40506, United States

Supporting Information

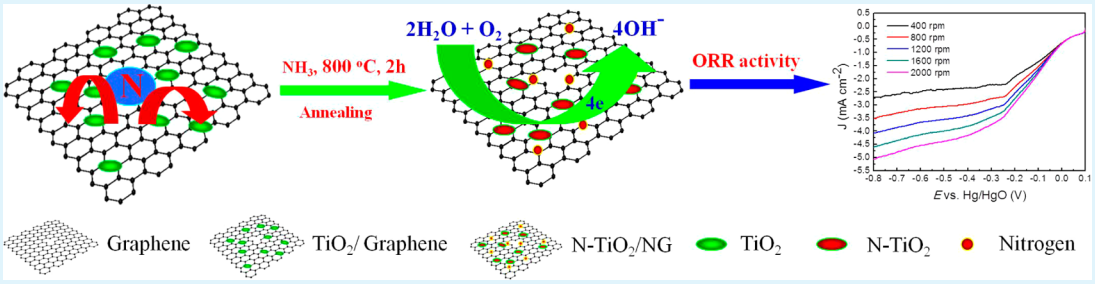

ABSTRACT: Developing an effective electrocatalyst for the oxygen reduction reaction is a momentous issue in fuel cells. In this paper, we successfully synthesized the N-doped TiO_2 nanorods/graphene (N-TiO_2/NG) nanocomposite, which comprise the N-doped TiO_2 (N-TiO_2) nanorods (40−60 nm diameter and 90−300 nm length) and self-assembled nitrogen-doped graphene (NG) networks. We found that the nanocomposite exhibits great oxygen reduction reaction (ORR) electrocatalytic performance and also shows long durability and methanol tolerance than that of the commercial 20% Pt/C catalyst. This new nanocomposite may also have potential applications in other fields, which are related to energy storage, gas sensors, photocatalysis, and so on.

KEYWORDS: *N-doped TiO_2, nitrogen-doped graphene, oxygen reduction reaction, nanocomposite*

1. INTRODUCTION

The oxygen reduction reaction (ORR) is a momentous issue in fuel cells.[1−3] So far, the best ORR catalyst still is the Pt-based material.[4] However, the intrinsical scarcity of Pt leads to the high cost and limits the mass-production and commercialization of these catalysts.[2,5,6] Considerable attention has therefore been paid to overcome the above problem by developing low-Pt or Pt-free catalysts for ORR.[7−10]

Recently, titanium dioxide (TiO_2) has been extensively studied as a photocatalyst in environmental protection and energy conversion.[11−16] However, as a kind of ORR catalyst, TiO_2 has rarely been studied, because the low conductivity remarkably restrains their practical application for ORR catalysts. Therefore, the strategies of the doping of TiO_2 with some heteroatoms have been taken.[17,18] For instance, developing the doping of TiO_2 with nitrogen (N-TiO_2) is an interesting approach. Because of the high abundance, N-TiO_2 is one of the most appealing electrocatalysts and appropriate for mass production.[19,20]

Recently, the nitrogen-doped (N-doped) carbon materials were reported to have the ability to improve the electron mobility and create favorable catalyst−support interactions, thus greatly promoting the catalyst's activity and stability for ORR.[8,21−25] Among them, graphene, composed of sp^2-hybridized carbon atoms, is very suitable for electric catalyst for ORR due to its high conductivity and outstanding mechanical properties.[26,27] For example, the nitrogen-doped graphene (NG) has become one of the most hottest topics in the electrocatalysts for fuel cells.[28,29] The NG has shown good catalytic ability, tolerance to the fuel molecule in the ORR process.[30−34] However, these N-doped materials still revealed lower catalytical ability compared to Pt-based catalysts. To further improve the performance of NG catalysts, much attention has been concentrated on the design of metallic oxide/NG or metal chalcogenides/NG nanocomposite with unique architectures to enhance ORR activity. Considering that these nanocomposites have quite good ORR activities, it is still challenging work to research the cost-effective metallic oxide or metal chalcogenides and NG for the high-performance of the ORR catalysts.[35−38]

Herein, we successfully synthesized the N-doped TiO_2 nanorods/graphene (N-TiO_2/NG) nanocomposite, comprising N-TiO_2 nanorods (40−60 nm diameter and 90−300 nm length) and self-assembled NG networks. The method is very suitable for large-scale production. Compared with N-TiO_2 or NG, the nanocomposite shows excellent catalytic activity for ORR. At the same time, the nanocomposite also shows long durability and methanol tolerance compared to that of the commercial 20% Pt/C. Due to these outstanding features, it is

Received: July 15, 2014
Accepted: November 18, 2014
Published: November 18, 2014

Scheme 1. Schematics of the Preparation of the N-TiO_2/NG Nanocomposite

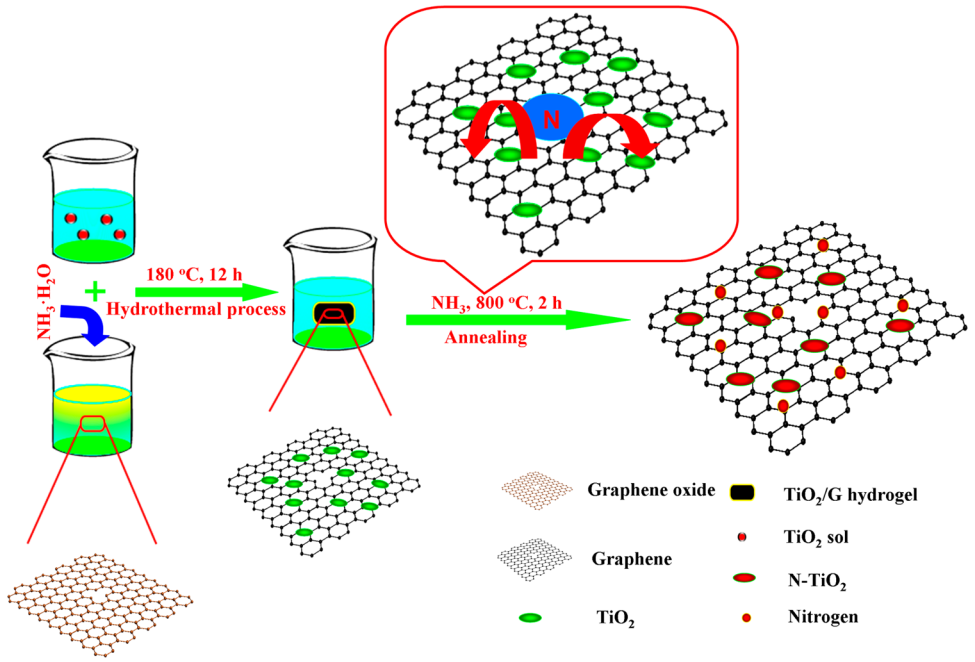

expected that the as-prepared N-TiO_2/NG will be a very suitable catalyst for the fuel cells.

2. EXPERIMENTAL SECTION

2.1. Materials. $KMnO_4$ (A.R.), H_2SO_4 (95−98%), $C_4H_{11}NO_2$ (A.R.), H_2O_2 (30%), and $NaNO_3$ (A.R.) were purchased from Shanghai chemical reagent factory (Shanghai, P. R. China). $C_{12}H_{28}O_4Ti$ (98%) was purchased from Aladdin industrial corporation (Shanghai, P. R. China). Graphite flakes were bought from Sigma-Aldrich Company.

2.2. Synthesis of the N-TiO_2/NG Nanocomposite. TiO_2 sol was prepared by the following procedure: 5.2 mL of titanium isopropoxide (TI) was dissolved in ethanol (32 mL) to yield TI solution. Then, 1.1 mL of diethanolamine was slowly added into the TI solution to form the TiO_2 sol by magnetic stirring for 24 h. Graphene oxide (GO) was prepared through the modified Hummer's method.[39] 2.56 mg mL^{-1} GO aqueous solution was used in the preparation.

The typical N-TiO_2/NG nanocomposite was prepared by the following procedure: 0.4 mL of TiO_2 sol was added into the mixture of 1.5 mL of $NH_3 \cdot H_2O$ and 20 mL of GO in a beaker at room temperature. After being stirred for 2 h, the mixtures were hydrothermally treated at 180 °C for 12 h. After the autoclave cooled down, the product was washed by DI water for several times and freeze-dried for 3 days to produce a TiO_2/graphene composite. Finally, the composite was annealed at 800 °C for 2 h in a tube furnace under NH_3 atmosphere, and the final product was obtained. The preparation procedure is shown in Scheme 1. For simplicity, according to the amount of the TiO_2 sol (0.2, 0.4, and 0.6 mL), the samples were denoted as N-TiO_2/NG-0.2, N-TiO_2/NG-0.4, and N-TiO_2/NG-0.6, respectively. N-TiO_2 was synthesized through the same steps as N-TiO_2/NG-0.4 without adding GO in the process, and NG was synthesized through the same steps as N-TiO_2/NG-0.4 without adding TiO_2 sol in the process.[40]

2.3. Characterization. Scanning transmission electronic microscopy (STEM) and field emission scanning electron microscopy (FE-SEM) images were recorded on a JEM-2100F instrument and Hitachi S4800-F high-resolution SEM. X-ray diffraction (XRD) measurements were preformed on a Philips X'Pert PRO SUPER X-ray diffractometer. X-ray photoelectron spectroscopic measurements (XPS) were performed on an X-ray photoelectron spectrometer (Escalon MKII). Raman spectra were performed on a Renishaw System 2000 spectrometer with a 532 nm laser excitation. The electrical conductivity of the sample was measured by a four-point measurement (ST2253, Suzhou Jingge Electronic Co., LTD, China).

2.4. Electrochemical Measurements. For electrochemical measurements, 10.0 mg of the catalyst was ultrasonically dispersed in the ethanol solution (5.0 mL) for 30 min. Then, a 5 μL mixture was dispersed onto the rotating glassy carbon electrode. Finally, a 5 μL Nafion solution (0.05 wt %) was adhered on the electrode and dried thoroughly in air. The commercial Pt/C catalyst (Johnson-Matthey Company, 20%) of 2 mg mL^{-1} was made by the same process. A CHI852C electrochemical workstation was used. A Pt wire and a Hg/HgO was used as the counter and reference electrodes, respectively. The voltammograms of the modified glassy carbon electrode were recorded in O_2-saturated 0.1 M KOH. The transferred electron number (n) in ORR was calculated from the Koutecky−Levich (K-L) equation.

$$\frac{1}{i} = \frac{1}{i_k} + \frac{1}{B\omega^{1/2}} \tag{1}$$

where i_k is the kinetic current and ω is the electrode rotating speed in rpm. B is Levich slope which is given by

$$B = 0.2nFC_{O_2}D_{O_2}^{2/3}\nu^{-1/6} \tag{2}$$

where n stands for the number of electrons transferred per oxygen molecule, F = 96 485 C mol^{-1} (Faraday constant), D_{O2} = 1.90 × 10^{-5} cm^2 s^{-1} (diffusion coefficient of O_2 in 0.1 M KOH), ν = 0.01 cm^2 s^{-1} (kinetic viscosity in 0.1 M KOH), and C_{O_2} = 1.2 × 10^{-6} mol cm^{-3} (concentration of O_2 in 0.1 M KOH).[41,42]

A rotating ring disk electrode system (RRDE) was used to measure the peroxide percentage (% H_2O_2) and electron transfer number (n). The % H_2O_2 and n were determined by the following equations:

$$\%H_2O_2 = 200 \times \frac{I_r/N}{I_d + I_r/N} \tag{3}$$

$$n = 4\frac{I_d}{I_d + I_r/N} \tag{4}$$

where I_d was the disk current, I_r was the ring current, and N is 0.35 (standing for the current collection efficiency of the Pt ring).[37]

3. RESULTS AND DISCUSSION

From Figure 1a,b, the N-TiO_2/NG nanocomposite contains many nanorods and graphene sheets. It can be observed that

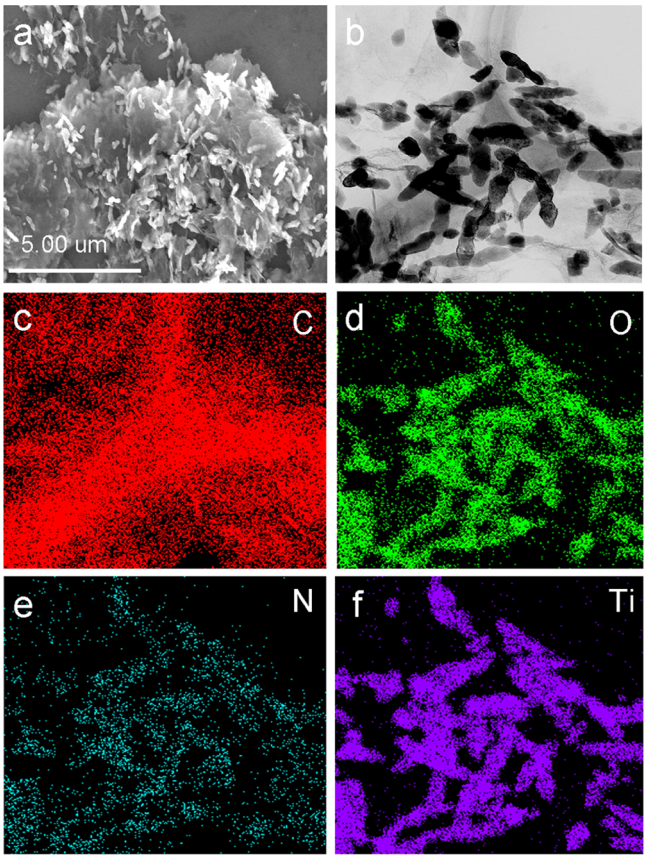

Figure 1. SEM image (a), STEM image of N-TiO_2/NG-0.4 (b), and corresponding element mapping images of (c–f) C, O, N, and Ti.

the nanorods exist homogeneously in the whole NG without obvious aggregation and their size is in the range of 40–60 nm in diameter and 90–300 nm in length. The scanning transmission electron microscopy (STEM) image and corresponding elemental mapping images show that the elements C, O, N, and Ti are distributed in the sample (Figure 1b–f). As shown in Figure 1d–f, the Ti signal and main O signal are overlaid with each other. In other words, the TiO_2 was dispersed in the nanocomposite. Very importantly, the part N signal is also overlaid with the main O signal and Ti signal. Therefore, we believe that the TiO_2 dispersed in the nanocomposite was doped by the nitrogen element. Certainly, the part N signal is also observed in the graphene, which means the graphene in the nanocomposite was also doped by the nitrogen element. Meanwhile, from the Figure S1 in the Supporting Information, EDX results also show that C, O, N, and Ti exist in the product.

The typical SEM image of the NG was shown in the Figure S2a (see the Supporting Information), which shows the NG has a highly wrinkled nature. The typical SEM images of the N-TiO_2/NG-0.2 and N-TiO_2/NG-0.6 were shown in the Figure S2b,c (see the Supporting Information).

Figure 2a shows the X-ray powder diffraction (XRD) patterns of the NG and N-TiO_2/NG-0.4. The diffraction peaks for N-TiO_2/NG-0.4 appeared at 25.3°, 37.7°, 48.0°, 55.1°, and 62.7°, corresponding to the (101), (004), (200), (211), and (204) crystal faces of TiO_2 (JCPDS card no. 04-0477), respectively. One major peak for NG and N-TiO_2/NG-0.4 appearing at about 26.4° can be assigned to the diffraction of graphene.[43] Therefore, the N-TiO_2/NG-0.4 presents a two-phase composition of N-TiO_2 and NG. The sample was analyzed by XPS analysis. As shown in Figures 2b–e and S3 (see the Supporting Information), the XPS spectra for N-TiO_2/NG-0.4 clearly indicate the incorporation of nitrogen and titanium atoms in the graphene. The C 1s XPS spectra afford four peaks at 284.7, 285.9, 286.5, and 287.8 eV for N-TiO_2/NG-0.4 (Figure 2b). The main peak at around 284.7 eV reflects the sp^2-hybridized carbon, while the small peaks at 285.9, 286.5, and 287.8 eV correspond to the existence of C–N, C–O, and C═O bonds.[44] The high-resolution O 1s XPS spectra of N-TiO_2/NG-0.4 (Figure 2c) present three peaks at 529.7, 531.4, and 532.4 eV. The dominant peak at 529.7 eV belongs to O 1s in the O–Ti linkage of TiO_2. The peak at around 532.4 eV can be ascribed to C–OH. The peak at 531.4 eV is attributed to O 1s in the Ti–O–N linkage, suggesting that the TiO_2 lattice laced into the nitrogen atom.[38,45,46] According to the literature, the binding energies of Ti $2p_{3/2}$ and Ti $2p_{1/2}$ for the pure TiO_2 sample are 459.1 and 465.0 eV, respectively.[45] Compared with the pure TiO_2 sample, the N-TiO_2/NG-0.4 shows a decrease of 0.3 eV (Figure 2d), suggesting the presence of Ti^{3+} and confirms that the nitrogen atom is doped into the TiO_2 lattice and is substituted for oxygen. Figure 2e shows the high-resolution N 1s spectra. Four peaks at 398.2, 398.6, 400.0, and 401.3 eV were observed. The peak located at 398.2 eV reflects the O–Ti–N bond formed by substitution for the oxygen atoms in the TiO_2 lattice.[47] Meanwhile, the other three peaks located at 398.6, 400.0, and 401.3 eV can be ascribed to the pyridinic N, pyrrolic N, and quaternary N, suggesting that the nitrogen atom was successfully doped.[44] On the basis of the above results, it can be considered that N-TiO_2/NG-0.4 has been formed. Figure 2f gives the Raman spectra of NG and N-TiO_2/NG-0.4, which exhibit two remarkable peaks around 1360 and 1590 cm^{-1}. They are assigned to D and G peaks of the graphene component. Meanwhile, a small broad peak was observed at around 2500–3000 cm^{-1} that corresponds to the 2D peak of graphene, suggesting that the graphene component in the N-TiO_2/NG-0.4 is a few layers.[48]

The electrocatalytic activities of the commercial Pt/C, NG, N-TiO_2, N-TiO_2/NG-0.2, N-TiO_2/NG-0.4, and N-TiO_2/NG-0.6 were tested. Figure 3a shows the corresponding rotating disc electrode (RDE) results. From Figure 3a, it is clear that the ORR onset potential and half-wave potential of N-TiO_2/NG-0.4 (5.0 mV, −70.0 mV) is more positive than that of NG (−130.0 mV, −250.0 mV) and N-TiO_2 (−235.0 mV, −310.0 mV), respectively. In addition, the current density (e.g., at −0.8 V vs Hg/HgO) of N-TiO_2/NG-0.4 (4.70 mA cm^{-2}) is also remarkably higher than that of NG (3.28 mA cm^{-2}) and N-TiO_2 (2.85 mA cm^{-2}). Compared with N-TiO_2 nanorods or NG, the N-TiO_2/NG-0.4 exhibits greatly enhanced electrocatalytic performance. Therefore, we believe that the remarkable catalytic activity of N-TiO_2/NG-0.4 can be ascribed to the appropriate N-TiO_2 in the nanocomposite. The ORR onset and half-wave potential of N-TiO_2/NG-0.4 (5.0 mV, −70.0 mV) is more positive than that of N-TiO_2/NG-0.2 (−40.0 mV, −150.0 mV) and N-TiO_2/NG-0.6 (−50.0 mV, −160.0 mV). Further, the linear sweep voltammograms on the N-TiO_2/NG-0.4 electrode were recorded at different rotating speeds (400–2000 rpm) in 0.1 M KOH. For comparison, the curves were also obtained for NG, N-TiO_2/NG-0.2, N-TiO_2/

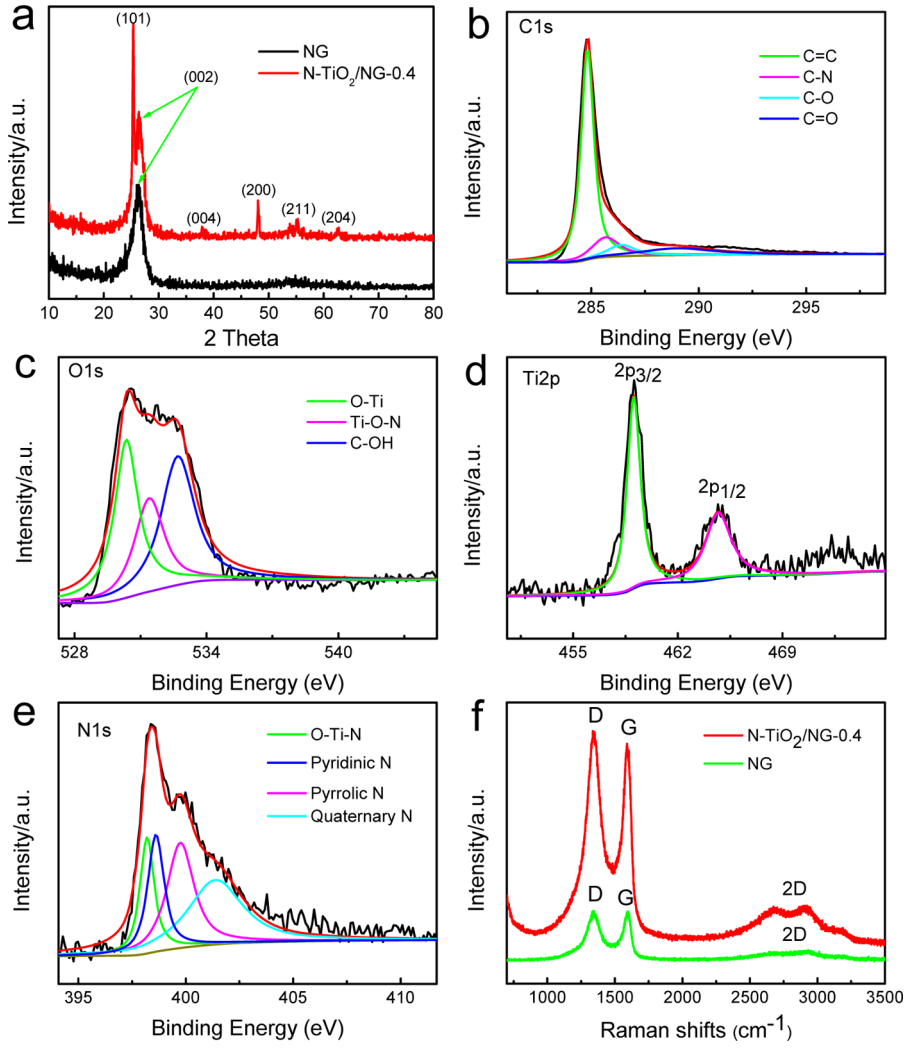

Figure 2. XRD patterns of NG and N-TiO_2/NG-0.4 (a). The high-resolution C 1s (b), O 1s (c), Ti 2p (d), and N 1s (e) XPS spectra. Raman spectra of N-TiO_2/NG-0.4 and NG catalysts (f).

NG-0.6, and commercial Pt/C (20 wt %) (see Figures 3b and S4 in the Supporting Information).[30] To qualify the ORR process, the K-L plots were obtained for N-TiO_2/NG-0.4 from the reaction currents at different potentials at various rotating speeds (Figure 3c). The K-L plots for NG, N-TiO_2/NG-0.2, N-TiO_2/NG-0.6, and commercial Pt/C were shown in the Figure S5 (see the Supporting Information).[49] The *n* values of all the samples were calculated by K-L eq 1. From Figure 3d, the N-TiO_2/NG-0.4 has the higher *n* value than those of NG, N-TiO_2/NG-0.2, and N-TiO_2/NG-0.6, suggesting that N-TiO_2/NG-0.4 exhibits an approximate four-electron reaction pathway. Nevertheless, the NG exhibits the *n* value of 3.68−3.40 according to the potentials, suggesting a combination of two- and four-electron pathways.

For practical applications, the stability of the catalysts is an important issue as well.[6,42,50] The stability of the N-TiO_2/NG-0.4 and commercial Pt/C was measured, respectively. The catalysts were held at −0.70 V for 18 000 s in 0.1 M KOH. From Figure 4a, the chronoamperometric response for N-TiO_2/NG-0.4 exhibiting the high relative current (85.2%) still persisted after 18 000 s. In contrast, the commercial Pt/C exhibiting the relative current (78.9%) persisted after 18 000 s. These results indicate the better stability of N-TiO_2/NG-0.4 than that of commercial Pt/C, which is suitable for the alkaline fuel cells. ORR polarization curves for N-TiO_2/NG-0.4 and commercial Pt/C in O_2-saturated 0.1 M KOH with and without 2.5 M CH_3OH were shown in Figure 4b. From Figure 4b, after the injection of methanol, no obvious change was observed at the N-TiO_2/NG-0.4 electrode, while for the commercial Pt/C, the remarkable decrease happened in the reduction current. These results clearly show the N-TiO_2/NG-0.4 catalyst has better tolerance to methanol poisoning effects and stability than the commercial Pt/C catalyst.

We also tested the performance for ORR by the RRDE system, and the amount of H_2O_2 generated could be accurately determined according to the eqs 3. Figure 5a shows the disk and ring currents for N-TiO_2/NG-0.4. From Figure 5b, the measured H_2O_2 yield for N-TiO_2/NG-0.4 was less than 7.5%. The electron transfer numbers were determined by eq 4 to be about 3.85 for our best catalysts (N-TiO_2/NG-0.4). Therefore, the ORR process at the N-TiO_2/NG-0.4 electrode belongs to a four-electron mechanism. Figure 5c,d shows the RRDE results of commercial Pt/C. The electron transfer number was approximately 3.95, and H_2O_2 yield was less than 7.3%. RRDE results of NG, N-TiO_2/NG-0.2, and N-TiO_2/NG-0.6 were shown in the Figure S6 (see the Supporting Information).

From the above discussion and the literature reported,[9,26,30,36,38,51] the nanocomposite shows great ORR

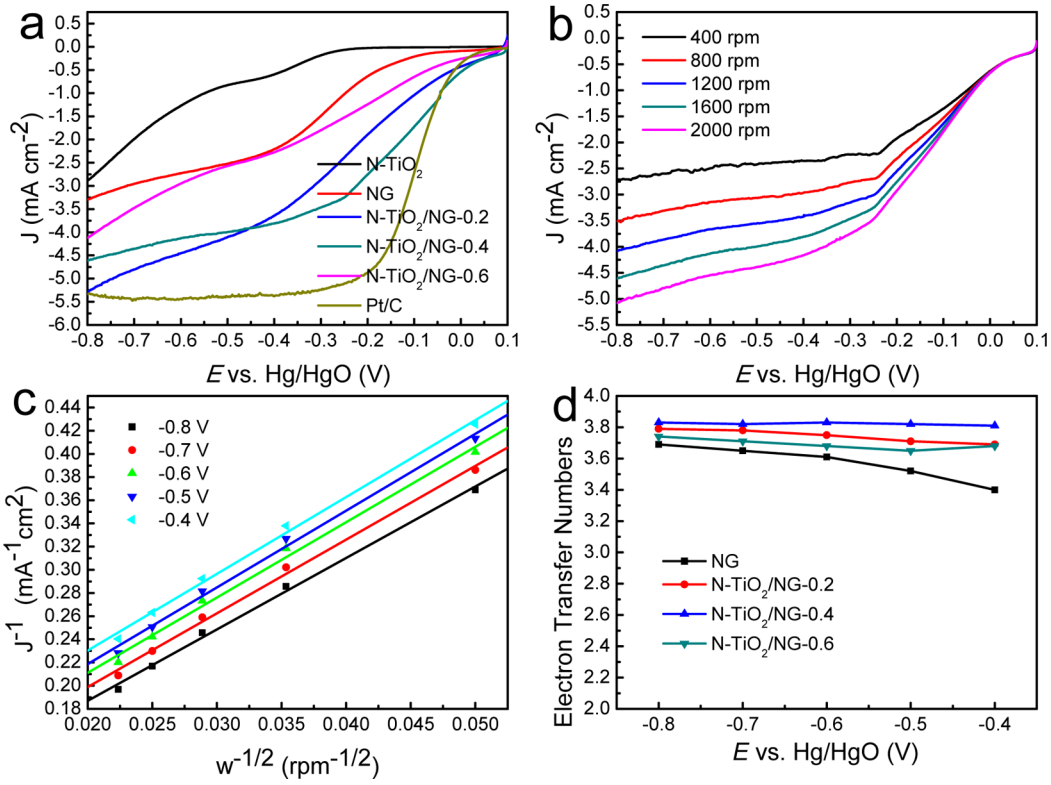

Figure 3. ORR polarization curves for N-TiO_2, NG, N-TiO_2/NG-0.2, N-TiO_2/NG-0.4, N-TiO_2/NG-0.6, and commercial Pt/C catalysts recorded in an O_2-saturated 0.1 M KOH (20 mV s^{-1}, 1600 rpm) (a), ORR curves for N-TiO_2/NG-0.4 catalyst at the different rotation rates indicated (b), K-L plots for the N-TiO_2/NG-0.4 catalyst at different potentials (c), electron transfer number of NG, N-TiO_2/NG-0.2, N-TiO_2/NG-0.4, and N-TiO_2/NG-0.6 as functions of the electrode potential (d), respectively.

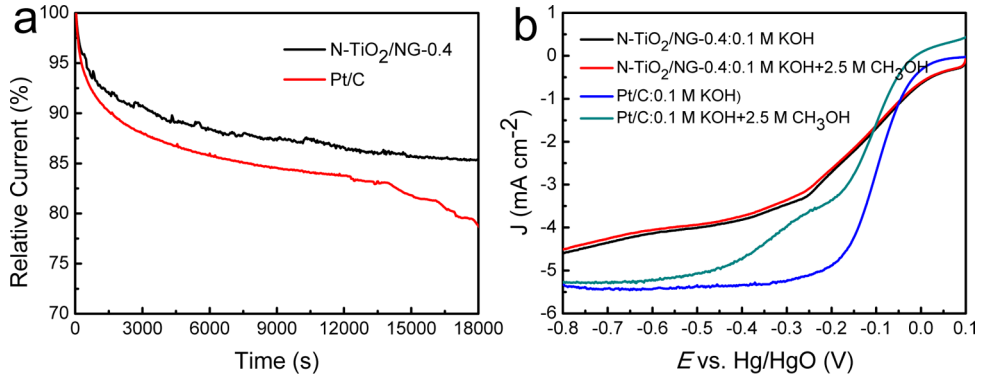

Figure 4. Chronoamperometric responses of N-TiO_2/NG-0.4 and commercial Pt/C catalysts at −0.70 V in O_2-saturated 0.1 M KOH (a) and ORR curves for N-TiO_2/NG-0.4 and commercial Pt/C in a 0.1 M KOH solution with and without 2.5 M CH_3OH (b), respectively.

electrocatalytic performance probably because of the N-doping and appropriate amount of N-TiO_2 in the nanocomposite. First, according to the literature,[22,24,26,28,31,52] N-doping can improve the electron-donor property and electron density of the graphene and reduce binding energy to break the O−O bonds for the oxygen molecules. Thus, doping of nitrogen plays an important role in ORR. Second, Figure 3a shows that the NG exists in the remarkably high activity unlike N-TiO_2. The main ORR active sites of N-TiO_2/NG-0.4 should be located in the NG. It is very significant to control the amount of N-TiO_2. A certain amount of N-TiO_2 nanorods can effectively prevent the restack of graphene sheets, leading to full exposure of the active sites of the sample and further enhancing the ORR activity. However, the inadequate amount of N-TiO_2 nanorods (see Figure S2b in the Supporting Information) cannot effectively prevent the NG sheets restacking, which will prevent the exposure of the active sites. An excess of N-TiO_2 nanorods (see Figure S2c in the Supporting Information) will lower the active sites of unit mass of the catalyst. Therefore, the N-TiO_2/NG-0.4 can effectively avoid the catalytic activity decrease and shows a wonderful performance. In addition, we found the conductivity of N-TiO_2 has greatly improved ($\rho_{N\text{-}TiO2} = 0.29\rho_{TiO2}$) compared to the TiO_2 (see the Supporting Information). The improved conductivity of N-TiO_2 should be helpful for the ORR performance.

4. CONCLUSIONS

We have successfully synthesized the N-TiO_2/NG nanocomposite, comprising N-TiO_2 nanorods and self-assembled

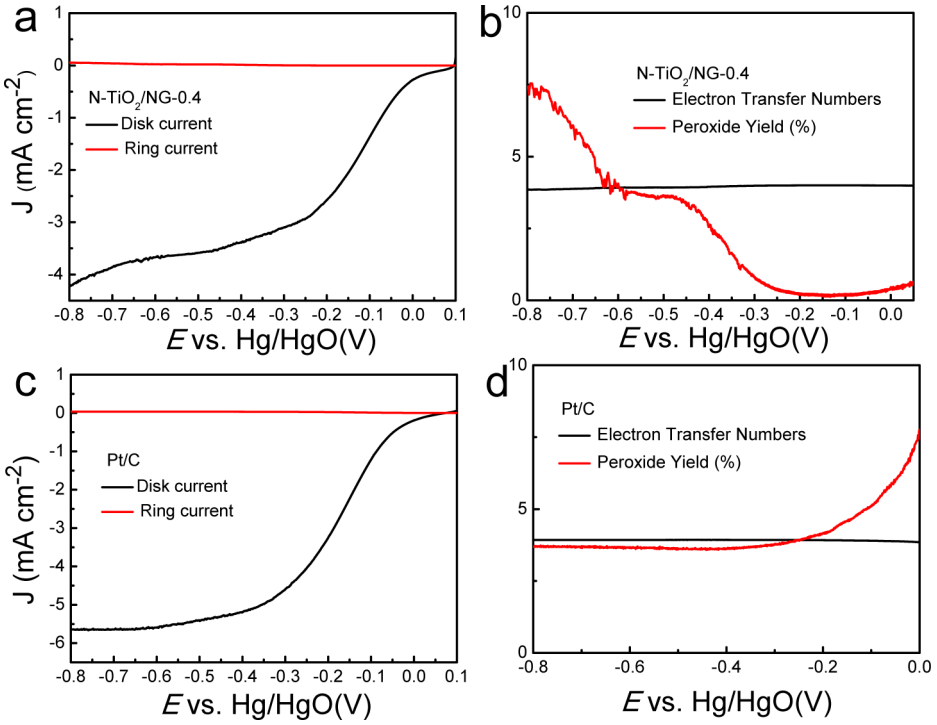

Figure 5. RRDE test of the ORR on (a) N-TiO_2/NG-0.4 and (c) commercial Pt/C catalysts in an O_2-saturated 0.1 M KOH (1600 rpm). The *n* and H_2O_2 yield of (b) N-TiO_2/NG-0.4 and (d) commercial 20% Pt/C catalysts as functions of the electrode potential.

nitrogen-doped graphene networks. Compared with N-TiO_2 nanorods or NG, the nanocomposite shows great ORR electrocatalytic performance because of the N-doping and appropriate amount of N-TiO_2 in the nanocomposite. The product also presents long durability and methanol tolerance compared to that of the commercial Pt/C (20%). It may have potential applications in the many fields such as energy storage, gas sensors, photocatalysis, etc. The synthesis method of N-TiO_2/NG may be used to synthesize other graphene-based nanocomposites.

■ ASSOCIATED CONTENT

Supporting Information

EDX results of N-TiO_2/NG-0.4. SEM images of NG, N-TiO_2/NG-0.2, and N-TiO_2/NG-0.6. XPS survey of the N-TiO_2/NG-0.4. ORR polarization curves for NG, N-TiO_2/NG-0.2, N-TiO_2/NG-0.6, and commercial Pt/C catalysts recorded in an O_2-saturated 0.1 M KOH at the different rotation rate. K-L plots for NG, N-TiO_2/NG-0.2, N-TiO_2/NG-0.6, and commercial Pt/C at different potentials. RRDE test of the ORR on NG, N-TiO_2/NG-0.2, and N-TiO_2/NG-0.6 in an O_2-saturated 0.1 M KOH (1600 rpm). This material is available free of charge via the Internet at http://pubs.acs.org.

■ AUTHOR INFORMATION

Corresponding Authors

*E-mail: chenping@ahu.edu.cn. Fax: +86-0551-63861475.
*E-mail: yhshen@ahu.edu.cn. Fax: +86-0551-63861475.

Notes

The authors declare no competing financial interest.

■ ACKNOWLEDGMENTS

The authors acknowledge the funding support from the National Natural Science Foundation of China (21271005, 91022032, 21173001, and 21371003) and Project of Science and Technology Head Introduction of Anhui University (02303203-0054).

■ REFERENCES

(1) Stamenkovic, V. R.; Fowler, B.; Mun, B. S.; Wang, G.; Ross, P. N.; Lucas, C. A.; Marković, N. M. Improved Oxygen Reduction Activity on Pt_3Ni (111) via Increased Surface Site Availability. *Science* **2007**, *315*, 493−497.

(2) Gong, K.; Du, F.; Xia, Z.; Durstock, M. Nitrogen-Doped Carbon Nanotube Arrays with High Electrocatalytic Activity for Oxygen Reduction. *Science* **2009**, *323*, 760−764.

(3) Xiong, W.; Du, F.; Liu, Y.; Perez, A., Jr.; Supp, M.; Ramakrishnan, T. S.; Dai, L.; Jiang, L. 3-D Carbon Nanotube Structures Used as High Performance Catalyst for Oxygen Reduction Reaction. *J. Am. Chem. Soc.* **2010**, *132*, 15839−15841.

(4) Lim, B.; Jiang, M.; Camargo, P. H.; Cho, E. C.; Tao, J.; Lu, X.; Zhu, Y.; Xia, Y. Pd-Pt Bimetallic Nanodendrites with High Activity for Oxygen Reduction. *Science* **2009**, *324*, 1302−1305.

(5) Liang, Y.; Li, Y.; Wang, H.; Zhou, J.; Wang, J.; Regier, T.; Dai, H. Co_3O_4 Nanocrystals on Graphene as a Synergistic Catalyst for Oxygen Reduction Reaction. *Nat. Mater.* **2011**, *10*, 780−786.

(6) Yang, Z.; Yao, Z.; Li, G.; Fang, G.; Nie, H.; Liu, Z.; Zhou, X.; Chen, X. a.; Huang, S. Sulfur-Doped Graphene as an Efficient Metal-Free Cathode Catalyst for Oxygen Reduction. *ACS Nano* **2011**, *6*, 205−211.

(7) Parvez, K.; Yang, S.; Hernandez, Y.; Winter, A.; Turchanin, A.; Feng, X.; Müllen, K. Nitrogen-Doped Graphene and Its Iron-Based Composite as Efficient Electrocatalysts for Oxygen Reduction Reaction. *ACS Nano* **2012**, *6*, 9541−9550.

(8) Chen, S.; Bi, J.; Zhao, Y.; Yang, L.; Zhang, C.; Ma, Y.; Wu, Q.; Wang, X.; Hu, Z. Nitrogen-Doped Carbon Nanocages as Efficient Metal-Free Electrocatalysts for Oxygen Reduction Reaction. *Adv. Mater.* **2012**, *24*, 5593−5597.

(9) Liu, R.; Wu, D.; Feng, X.; Müllen, K. Nitrogen-Doped Ordered Mesoporous Graphitic Arrays with High Electrocatalytic Activity for Oxygen Reduction. *Angew. Chem., Int. Ed.* **2010**, *122*, 2619−2623.

(10) Yang, L.; Jiang, S.; Zhao, Y.; Zhu, L.; Chen, S.; Wang, X.; Wu, Q.; Ma, J.; Ma, Y.; Hu, Z. Boron-Doped Carbon Nanotubes as Metal-Free Electrocatalysts for the Oxygen Reduction Reaction. *Angew. Chem.* **2011**, *123*, 7270−7273.
(11) Albu, S. P.; Ghicov, A.; Macak, J. M.; Hahn, R.; Schmuki, P. Self-Organized, Free-Standing TiO_2 Nanotube Membrane for Flow-Through Photocatalytic Applications. *Nano Lett.* **2007**, *7*, 1286−1289.
(12) Zhang, H.; Lv, X.; Li, Y.; Wang, Y.; Li, J. P25-Graphene Composite as a High Performance Photocatalyst. *ACS Nano* **2009**, *4*, 380−386.
(13) Feng, X.; Shankar, K.; Varghese, O. K.; Paulose, M.; Latempa, T. J.; Grimes, C. A. Vertically Aligned Single Crystal TiO_2 Nanowire Arrays Grown Directly on Transparent Conducting Oxide Coated Glass: Synthesis Details and Applications. *Nano Lett.* **2008**, *8*, 3781−3786.
(14) Zhu, K.; Neale, N. R.; Miedaner, A.; Frank, A. J. Enhanced Charge-Collection Efficiencies and Light Scattering in Dye-Sensitized Solar Cells Using Oriented TiO_2 Nanotubes Arrays. *Nano Lett.* **2007**, *7*, 69−74.
(15) Bach, U.; Lupo, D.; Comte, P.; Moser, J.; Weissörtel, F.; Salbeck, J.; Spreitzer, H.; Grätzel, M. Solid-State Dye-Sensitized Mesoporous TiO_2 Solar Cells with High Photon-to-Electron Conversion Efficiencies. *Nature* **1998**, *395*, 583−585.
(16) Koo, H. J.; Kim, Y. J.; Lee, Y. H.; Lee, W. I.; Kim, K.; Park, N. G. Nano-Embossed Hollow Spherical TiO_2 as Bifunctional Material for High-Efficiency Dye-Sensitized Solar Cells. *Adv. Mater.* **2008**, *20*, 195−199.
(17) Elezović, N.; Babić, B.; Gajić-Krstajić, L.; Radmilović, V.; Krstajić, N.; Vračar, L. Synthesis, Characterization and Electrocatalytical Behavior of Nb−TiO_2/Pt Nanocatalyst for Oxygen Reduction Reaction. *J. Power Sources* **2010**, *195*, 3961−3968.
(18) Huang, K.; Sasaki, K.; Adzic, R. R.; Xing, Y. Increasing Pt Oxygen Reduction Reaction Activity and Durability with a Carbon-Doped TiO_2 Nanocoating Catalyst Support. *J. Mater. Chem.* **2012**, *22*, 16824−16832.
(19) Wang, W.; Savadogo, O.; Ma, Z.-F. The Oxygen Reduction Reaction on Pt/TiO_xN_y-Based Electrocatalyst for PEM Fuel Cell Applications. *J. Appl. Electrochem.* **2012**, *42*, 857−866.
(20) Chisaka, M.; Ishihara, A.; Suito, K.; Ota, K.-i.; Muramoto, H. Oxygen Reduction Reaction Activity of Nitrogen-Doped Titanium Oxide in Acid Media. *Electrochim. Acta* **2013**, *88*, 697−707.
(21) Tang, Y.; Allen, B. L.; Kauffman, D. R.; Star, A. Electrocatalytic Activity of Nitrogen-Doped Carbon Nanotube Cups. *J. Am. Chem. Soc.* **2009**, *131*, 13200−13201.
(22) Sharifi, T.; Hu, G.; Jia, X.; Wagberg, T. Formation of Active Sites for Oxygen Reduction Reactions by Transformation of Nitrogen Functionalities in Nitrogen-Doped Carbon Nanotubes. *ACS Nano* **2012**, *6*, 8904−8912.
(23) Wu, Z. S.; Winter, A.; Chen, L.; Sun, Y.; Turchanin, A.; Feng, X.; Müllen, K. Three-Dimensional Nitrogen and Boron Co-Doped Graphene for High-Performance All-Solid-State Supercapacitors. *Adv. Mater.* **2012**, *24*, 5130−5135.
(24) Wei, D.; Liu, Y.; Wang, Y.; Zhang, H.; Huang, L.; Yu, G. Synthesis of N-Doped Graphene by Chemical Vapor Deposition and Its Electrical Properties. *Nano Lett.* **2009**, *9*, 1752−1758.
(25) Zhou, X.; Wan, L. J.; Guo, Y. G. Binding SnO_2 Nanocrystals in Nitrogen-Doped Graphene Sheets as Anode Materials for Lithium-Ion Batteries. *Adv. Mater.* **2013**, *25*, 2152−2157.
(26) Qu, L.; Liu, Y.; Baek, J.-B.; Dai, L. Nitrogen-Doped Graphene as Efficient Metal-Free Electrocatalyst for Oxygen Reduction in Fuel Cells. *ACS Nano* **2010**, *4*, 1321−1326.
(27) Yang, S.; Feng, X.; Wang, X.; Müllen, K. Graphene-Based Carbon Nitride Nanosheets as Efficient Metal-Free Electrocatalysts for Oxygen Reduction Reactions. *Angew. Chem., Int. Ed.* **2011**, *50*, 5339−5343.
(28) Chen, P.; Xiao, T. Y.; Qian, Y. H.; Li, S. S.; Yu, S. H. A Nitrogen-Doped Graphene/Carbon Nanotube Nanocomposite with Synergistically Enhanced Electrochemical Activity. *Adv. Mater.* **2013**, *25*, 3192−3196.
(29) KokáPoh, C. Exploration of the Active Center Structure of Nitrogen-Doped Graphene-Based Catalysts for Oxygen Reduction Reaction. *Energy Environ. Sci.* **2012**, *5*, 7936−7942.
(30) Li, Q.; Zhang, S.; Dai, L.; Li, L.-S. Nitrogen-Doped Colloidal Graphene Quantum Dots and Their Size-Dependent Electrocatalytic Activity for the Oxygen Reduction Reaction. *J. Am. Chem. Soc.* **2012**, *134*, 18932−18935.
(31) Lin, Z.; Waller, G. H.; Liu, Y.; Liu, M.; Wong, C.-P. 3D Nitrogen-Doped Graphene Prepared by Pyrolysis of Graphene Oxide with Polypyrrole for Electrocatalysis of Oxygen Reduction Reaction. *Nano Energy* **2013**, *2*, 241−248.
(32) Liang, J.; Jiao, Y.; Jaroniec, M.; Qiao, S. Z. Sulfur and Nitrogen Dual-Doped Mesoporous Graphene Electrocatalyst for Oxygen Reduction with Synergistically Enhanced Performance. *Angew. Chem., Int. Ed.* **2012**, *51*, 11496−11500.
(33) Wang, S.; Zhang, L.; Xia, Z.; Roy, A.; Chang, D. W.; Baek, J. B.; Dai, L. BCN Graphene as Efficient Metal-Free Electrocatalyst for the Oxygen Reduction Reaction. *Angew. Chem., Int. Ed.* **2012**, *51*, 4209−4212.
(34) Zhang, L.; Niu, J.; Dai, L.; Xia, Z. Effect of Microstructure of Nitrogen-Doped Graphene on Oxygen Reduction Activity in Fuel Cells. *Langmuir* **2012**, *28*, 7542−7550.
(35) Bag, S.; Roy, K.; Gopinath, C. S.; Raj, C. R. A Facile Single-Step Synthesis of Nitrogen-Doped Reduced Graphene Oxide-Mn_3O_4 Hybrid Functional Material for the Electrocatalytic Reduction of Oxygen. *ACS Appl. Mater. Interfaces* **2014**, *6*, 2692−2699.
(36) Yuan, W.-J.; Li, J.-C.; Chen, P.; Shen, Y.-H.; Xie, A.-J. A One-Pot Hydrothermal Synthesis of 3D Nitrogen-Doped Graphene Aerogels-Supported NiS_2 Nanoparticles as Efficient Electrocatalysts for the Oxygen-Reduction Reaction. *J. Nanopart. Res.* **2014**, *16*, 1−8.
(37) Wu, Z.-S.; Yang, S.; Sun, Y.; Parvez, K.; Feng, X.; Müllen, K. 3D Nitrogen-Doped Graphene Aerogel-Supported Fe_3O_4 Nanoparticles as Efficient Electrocatalysts for the Oxygen Reduction Reaction. *J. Am. Chem. Soc.* **2012**, *134*, 9082−9085.
(38) Chen, P.; Xiao, T.-Y.; Li, H.-H.; Yang, J.-J.; Wang, Z.; Yao, H.-B.; Yu, S.-H. Nitrogen-Doped Graphene/ZnSe Nanocomposites: Hydrothermal Synthesis and Their Enhanced Electrochemical and Photocatalytic Activities. *ACS Nano* **2011**, *6*, 712−719.
(39) Hummers, W. S., Jr.; Offeman, R. E. Preparation of Graphitic Oxide. *J. Am. Chem. Soc.* **1958**, *80*, 1339−1339.
(40) Xu, Y.; Sheng, K.; Li, C.; Shi, G. Self-Assembled Graphene Hydrogel via a One-Step Hydrothermal Process. *ACS Nano* **2010**, *4*, 4324−4330.
(41) Davis, R.; Horvath, G.; Tobias, C. The Solubility and Diffusion Coefficient of Oxygen in Potassium Hydroxide Solutions. *Electrochim. Acta* **1967**, *12*, 287−297.
(42) Yin, H.; Tang, H.; Wang, D.; Gao, Y.; Tang, Z. Facile Synthesis of Surfactant-Free Au Cluster/Graphene Hybrids for High-Performance Oxygen Reduction Reaction. *ACS Nano* **2012**, *6*, 8288−8297.
(43) Jafri, R. I.; Rajalakshmi, N.; Ramaprabhu, S. Nitrogen Doped Graphene Nanoplatelets as Catalyst Support for Oxygen Reduction Reaction in Proton Exchange Membrane Fuel Cell. *J. Mater. Chem.* **2010**, *20*, 7114−7117.
(44) Lee, K. R.; Lee, K. U.; Lee, J. W.; Ahn, B. T.; Woo, S. I. Electrochemical Oxygen Reduction on Nitrogen Doped Graphene Sheets in Acid Media. *Electrochem. Commun.* **2010**, *12*, 1052−1055.
(45) Xing, M.; Zhang, J.; Chen, F. New Approaches to Prepare Nitrogen-Doped TiO_2 Photocatalysts and Study on Their Photocatalytic Activities in Visible Light. *Appl. Catal., B* **2009**, *89*, 563−569.
(46) Wang, D.-H.; Jia, L.; Wu, X.-L.; Lu, L.-Q.; Xu, A.-W. One-Step Hydrothermal Synthesis of N-Doped TiO_2/C Nanocomposites with High Visible Light Photocatalytic Activity. *Nanoscale* **2012**, *4*, 576−584.
(47) Sathish, M.; Viswanathan, B.; Viswanath, R.; Gopinath, C. S. Synthesis, Characterization, Electronic Structure, and Photocatalytic Activity of Nitrogen-Doped TiO_2 Nanocatalyst. *Chem. Mater.* **2005**, *17*, 6349−6353.
(48) Yin, H.; Liu, S.; Zhang, C.; Bao, J.; Zheng, Y.; Han, M.; Dai, Z. Well-Coupled Graphene and Pd-Based Bimetallic Nanocrystals

Nanocomposites for Electrocatalytic Oxygen Reduction Reaction. *ACS Appl. Mater. Interfaces* **2014**, *6*, 2086−2094.
(49) Lin, Z.; Waller, G.; Liu, Y.; Liu, M.; Wong, C. P. Facile Synthesis of Nitrogen-Doped Graphene via Pyrolysis of Graphene Oxide and Urea, and Its Electrocatalytic Activity toward the Oxygen-Reduction Reaction. *Adv. Energy Mater.* **2012**, *2*, 884−888.
(50) Peng, H.; Mo, Z.; Liao, S.; Liang, H.; Yang, L.; Luo, F.; Song, H.; Zhong, Y.; Zhang, B. High Performance Fe-and N-Doped Carbon Catalyst with Graphene Structure for Oxygen Reduction. *Sci. Rep.* **2013**, *3*, 1−7.
(51) Sheng, Z.-H.; Gao, H.-L.; Bao, W.-J.; Wang, F.-B.; Xia, X.-H. Synthesis of Boron Doped Graphene for Oxygen Reduction Reaction in Fuel Cells. *J. Mater. Chem.* **2012**, *22*, 390−395.
(52) Chen, P.; Wang, L. K.; Wang, G.; Gao, M. R.; Ge, J.; Yuan, W. J.; Shen, Y. H.; Xie, A. J.; Yu, S. H. Nitrogen-Doped Nanoporous Carbon Nanosheets Derived from Plant Biomass: An Efficient Catalyst for Oxygen Reduction Reaction. *Energy Environ. Sci.* **2014**, DOI: 10.1039/C4EE02531H.